Cellular flow patterns and their evolutionary scenarios in three-dimensional Rayleigh-Bénard convection

A. V. Getling*
Institute of Nuclear Physics, Lomonosov Moscow State University, 119992 Moscow, Russia

O. Brausch
Institute of Physics, University of Bayreuth, D-95440 Bayreuth, Germany
(Received 18 October 2002; published 29 April 2003)

The evolution of three-dimensional, cellular convective flows in a plane horizontal layer of a Boussinesq fluid heated from below is studied numerically. Slow motion in the form of a spatially periodic pattern of hexagonal cells is introduced initially. In a further development, the flow can undergo a sequence of transitions between various cell types. The features of the flow evolution agree with the idea of the flow seeking an optimal scale. In particular, two-vortex polygonal cells may form at some evolution stages, with an annular planform of the upflow region and downflows localized in both central and peripheral regions of the cells. If short-wave hexagons are stable, they exhibit a specific, stellate fine structure.

DOI: 10.1103/PhysRevE.67.046313 PACS number(s): 47.20.Ky, 47.27.Te, 47.54.+r

Quasi-two-dimensional roll flows are the most typical forms of convection in a plane horizontal fluid layer heated from below (Rayleigh-Bénard convection, RBC) over a wide range of Rayleigh numbers R, provided that the spatial distribution of the material parameters of the fluid does not exhibit any significant up-down asymmetry (asymmetry with respect to the horizontal midplane of the layer). However, three-dimensional cellular flows are not prohibited in symmetric layers and, as established in recent years, can be stable within a certain region of the parameter space. Stable hexagonal cells in a nearly uniform layer were experimentally observed by Assenheimer and Steinberg [1] at a strongly supercritical R. Subsequently, Clever and Busse [2] analyzed, in a linear approximation, the stability of finite-amplitude flows in the form of hexagonal cells. They found that a region of stable hexagonal-cell flow regimes exists in the (k,R) plane (where k is the horizontal wave number of the flow) at Prandtl numbers $P \gtrsim 1.2$. A stability region was also revealed for square cells asymmetric about the midplane [3,4]. Thus, at given parameter values, two or more attractors corresponding to different flow forms can in general coexist, although their basins of attraction in the space of initial states may differ widely in size.

Two-dimensional convective roll flows normally exhibit a tendency to approach a certain wave number, optimal under given conditions but not always achievable (see Ref. [5] for a detailed discussion). This optimum should also emerge in the three-dimensional cellular patterns. However, the transformations that can bring such patterns closer to the optimum still remain unexplored.

Here, we analyze such transformations in the RBC using spectral numerical simulations. At initial time, we specify a weak temperature-velocity perturbation in the form of a spatially periodic pattern of hexagonal cells. The wave number k_0 of this perturbation defines the periods of the pattern in the horizontal x and y directions. In most cases, precisely as in the stability analysis by Clever and Busse [2], we restricted ourselves to studying only such flow transformations that do not increase the fundamental wavelength of the pattern. Accordingly, the periods of the initially induced pattern in x and y directions were simultaneously the corresponding wavelengths of the lowest harmonic in the spectrum. However, a few additional computational runs were based on spectra whose lowest harmonics had double the spatial periods of the original pattern. We will denote them as d runs.

We adopt the standard formulation of the problem of the RBC (see, e.g., Ref. [5]). Specifically, the Navier-Stokes equation, the heat-diffusion equation, and the continuity equation are written in the Boussinesq approximation; no-slip, isothermal boundary conditions are imposed at the horizontal layer surfaces $z=0,1$ (the layer thickness is used here as the unit length).

In solving the problem, we use the technique proposed by Pesch (see Ref. [6] for a description). The velocity field is decomposed into a poloidal and a toroidal component, and a spectral (Galerkin) technique is applied to these two velocity components and temperature. The fields are expanded in the Fourier series in x and y, and the basis functions representing the z dependences are trigonometric functions for the temperature and the Chandrasekhar functions for velocity. The efficiency of the numerical algorithm is greatly enhanced by means of treating the time variation of higher harmonics in an adiabatic approximation, without numerical integrations. The behavior of the lower (''active'') modes is computed using the Adams-Bashforth method. For computations, we employ an adaptation of the numerical code developed by Pesch.

The parameters determining the scenario of evolution are R and P, as well as the wave number k_0 of the initially specified perturbation. We carried out our computations for $P=1$, 2.5, and 7. The last two values were chosen for the sake of direct comparability between our results and those of Clever and Busse [2].

The flow structures revealed in our simulations will be described below in terms of the distributions of temperature

*Electronic address: A.Getling@ru.net

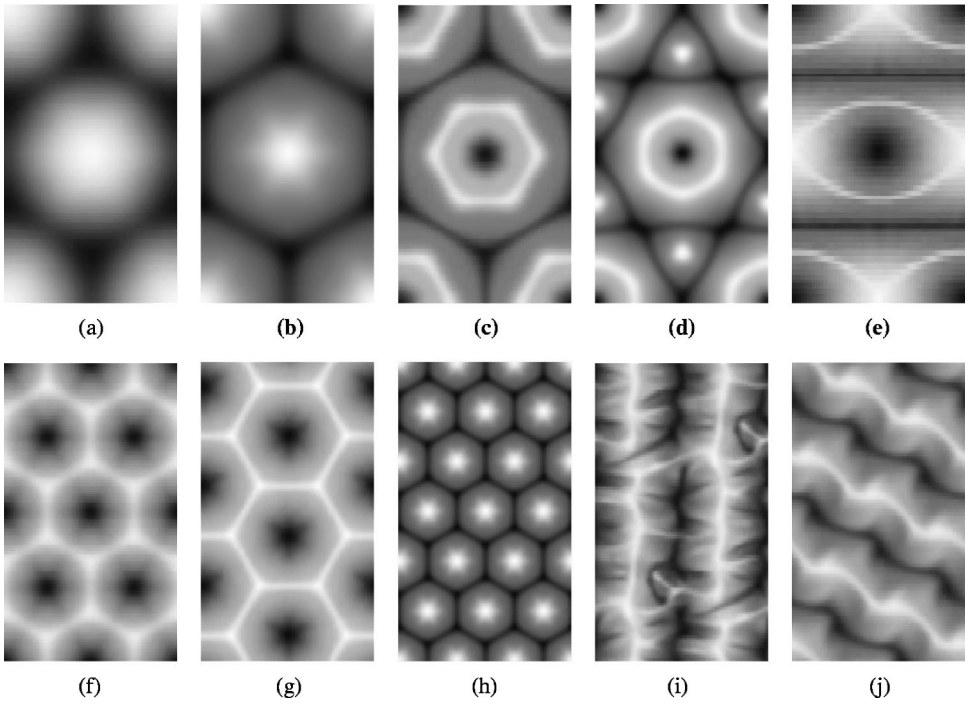

FIG. 1. Types of ultimately established structures [in all figures, temperature distributions are shown in a gray-scale representation, with the white regions warm and the black regions cold; here, as in Figs. 2(b) and 3, these distributions refer to the midplane $z=1/2$ of the layer]: (a) 1-cell, (b) stellate 1-cell, (c) ''perfect'' two-vortex cell, (d) small two-vortex cell with joining triangles, (e) eyed pattern, (f) 2-cells with inverse circulation, (g) $\sqrt{3}$-cells, (h) 3-cells with direct circulation, (i) unsteady rolls, (j) traveling waves.

perturbations over horizontal sections of the layer (mainly, over the midplane $z=1/2$). As known from numerous studies of convective phenomena, such a horizontal temperature distribution mimics, to a first approximation, the distribution of the vertical component of velocity over the same section.

Generally, the above-noted restriction on the wavelengths of the perturbations would prevent our computational scheme from describing a large-scale flow, if such a flow could arise. However, in the cases we consider, the generation of a mean drift is forbidden by the flow symmetry.

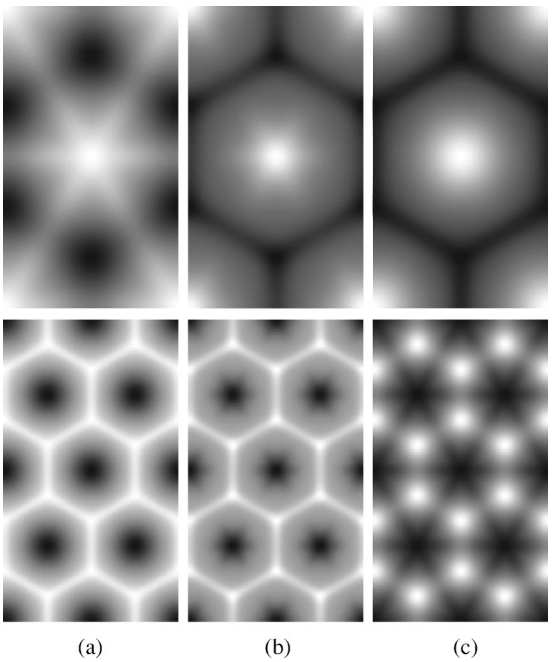

FIG. 2. Temperature fields in a stellate 1-cell (top: $R=12\,000$, $P=7$, $k_0=2.4$) and stellate 2-cells with inverse circulation (bottom: $R=14\,000$, $P=2.5$, $k_0=1.2$) at levels of (a) $z=0.05$, (b) $z=0.5$, and (c) $z=0.95$.

First of all, our findings agree with the results of the linear stability analysis [2]. If k_0 is within the stability band, stable hexagons with a wave number $k=k_0$ develop from the initial perturbation [Fig. 1(a)], we will call them 1-cells. The same situation takes place if the initial wave number is beyond the short-wave boundary of the stability band. The point is that the merger of small, high-k_0 cells into larger cells is forbidden in our simulations, since k_0 coincides with the wave number of the lowest harmonic in the spectrum.

It is worth noting that the stable 1-cells that persist at high wave numbers, beyond the linear-stability boundary, exhibit a remarkable fine structure (some features of this sort can also be seen in Fig. 1 in Ref. [2]). The horizontal temperature distributions demonstrate stellate patterns: in each hexagonal cell, six warm rays stretch from the center to the vertices of the hexagon [Fig. 1(b)]. At $P=7$, such patterns are much more pronounced than at $P=2.5$; they are especially clear-cut in the lower boundary layer [Figs. 2(a) and 2(b), top]. Thus, a collection of radially stretched vortices, resembling convection rolls broadening toward the cell periphery, appear to be superposed onto the main circulation in the lower part of the cell. This pattern seems to be akin to crossed rolls in normal roll convection. In cells with inverse circulation, cool rays can be observed in the upper part of the layer [Figs. 2(b) and 2(c), bottom].

If the point representing the initial state in the (k,R) diagram is to the left of the long-wave boundary of the linear-stability region or, possibly, above the upper boundary of this region (as in the case of some runs for $P=2.5$), the originally induced hexagons are unstable and transform into other structures with smaller characteristic scales. The final wave number may lie either within the theoretical stability region or to the right of the short-wave boundary of this region. The

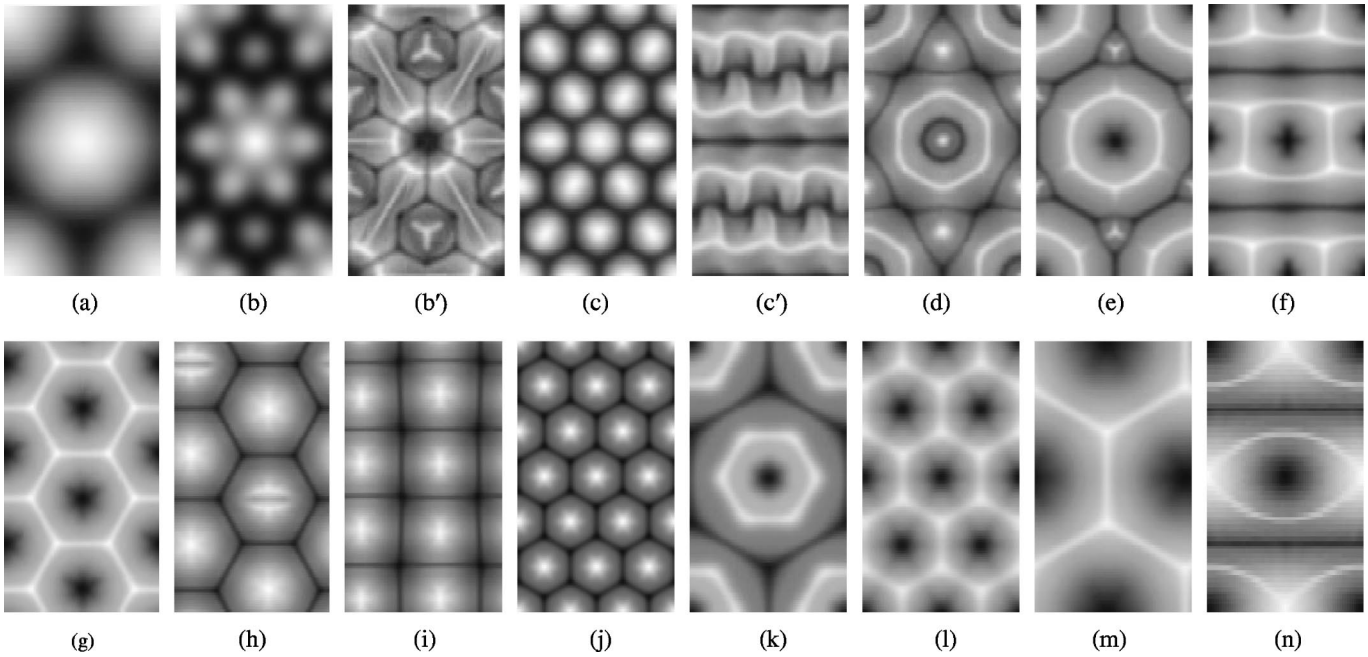

FIG. 3. Basic stages of the pattern evolution: (a) 1-cell, (b), (c) breakdown of the 1-cell into 3-cells, (b′) ''hydrodynamic kaleidoscope'' at the breakdown stage, (c′) traveling waves, (d) small two-vortex cell with joining triangles (transient form with a central umbilicus), (e) large two-vortex cell with joining triangles, (f) railway pattern, (g) $\sqrt{3}$-cells with inverse circulation; (h) ''chewing'' $\sqrt{3}$-cells with direct circulation, (i) square cells, (j) 3-cells with direct circulation, (k) perfect two-vortex cell, (l) 2-cells with inverse circulation, (m) 1-cells with inverse circulation, (n) eyed pattern.

specific value of the final wave number depends primarily on the expected optimum wave number; at the same time, a fairly wide spread around this optimum is present, since the spatial spectrum of the flow is discrete in our problem. Here, we only study qualitative features of the flow evolution rather than determine the particular wave numbers. Figure 1 shows some final states we observed.

In many cases, the flow arrives at a pattern of hexagonal cells smaller than the original ones. Depending on the optimum flow scale, they may be smaller than 1-cells by a factor of 2 [Figs. 1(f) and 2(a)–2(c)], $\sqrt{3}$ [Fig. 1(g)], or 3 [Fig. 1(h)]; we will call them 2-cells, $\sqrt{3}$-cells, or 3-cells, respectively. The 2-cells and $\sqrt{3}$-cells that develop from the 1-cells are characterized by inverse circulation: the fluid ascends in the peripheral regions of the cells and descends in their centers. The most peculiar types of finally established structures are intermediate in their characteristic scale between 1-cells and 2-cells. They can naturally be called two-vortex hexagonal cells [Figs. 1(c) and 1(d)], since each of them is formed by two closed concentric annular vortices surrounding the center of the cell: in any meridional section of the cell, an upflow region is present at a certain distance from the center, while two downflow regions are situated near the center and at the periphery of the cell.

No transformations into rolls took place at $P=2.5$ and 7. For $P=1$ and $k_0 \lesssim 1.2$, the flow arrived at a pattern of unsteady rolls; they varied their orientation [Figs. 1(i) and 1(j)], so that the roll width closest to the optimum value was chosen by the flow in any particular case out of the set of possible widths. In some cases, waves traveling along the rolls were observed [Fig. 1(j)].

Figure 1(e) shows one more peculiar type of the final state of the flow. It was observed in a *d* run for $R=18\,000$, $P=2.5$, and $k_0=1$. The pattern has a curious, ''eyed'' appearance in this case.

When describing evolutionary scenarios, we will refer to Fig. 3, marking particular stages of the evolution by the alphabets denoting the corresponding patterns in the figure. As noted above, we observed cell transformations if k_0 was less than the long-wave bounding wave number of the stability range. Most computational runs that demonstrate such transformations refer to $P=2.5$.

At small k_0 (~ 0.8 for $14\,000 < R < 18\,000$, $P=2.5$), the original cells disintegrate into 3 cells, which then settle down to a steady state: (a)→(b)→(c)→(j). The additional *d* run for $R=18\,000$ demonstrates, after the formation of 3-cells, a number of complex transformations, which ultimately lead to $\sqrt{3}$-cells with direct circulation: (a)→(b)→(c)→(j)→ $\cdots$ →(g)* (the asterisk indicates that the direction of circulation is opposite to that shown in Fig. 3). Thus, adding new degrees of freedom to the system facilitates the attainment of the final state with a wave number of $\sqrt{3}k_0$, which seems to be closer to the optimum value than $3k_0$ is.

At a larger Rayleigh number of $R=20\,000$ and the same k_0, the final state of the flow is time dependent, and $\sqrt{3}$-cells form ultimately. The final wave number is thus reduced as compared to the case of a smaller *R*. This agrees with the well-known general regularity that the optimum wave number of the RBC and, on an average, the final wave numbers reached in various particular situations decrease with increasing *R* (see, e.g., Ref. [5]). The following path is real-

ized: (a)→(b)→(c)→(j)→(i)→(h). The final state is represented by the cells with direct circulation. This pattern is characterized by the periodic alternation of broadening and narrowing of dark bars intersecting some cells; for this reason, we call them ''chewing'' cells.

In most regimes with unstable 1-cells, they rapidly break down into 3-cells. If $3k_0$ proves to be much larger than the optimum wave number, 3-cells (which may not be fully developed) combine to form two-vortex hexagons: (a)→(b)→(c) [→(d)]→(e)→··· [the square brackets mean that stage (d) can be skipped]. Furthermore, in some cases, e.g., at $k=1$ and $14\,000<R<20\,000$, such scenarios can be completed as follows: ···→(f)→(g). For $R=18\,000$ or $20\,000$, the final state (g) is time dependent, with vibrating cell boundaries; the additional *d* runs demonstrate a complex sequence of the transitions between states (c) and (n) for $R=18\,000$ and a steady (g) state for $R=20\,000$.

If $k=1.2$, the evolution leads to a final (l) state (2-cells) at $14\,000<R<18\,000$ and to a (k) state (''perfect'' two-vortex cells) at $R=20\,000$. If $k=1.4$, an (l) state is also typical of $R=14\,000$, while 1-cells are recovered at high R values. At $R=18\,000$, an inverse circulation (m) state was observed. This is obviously an accident, since both directions of circulation are equally probable in layers without an up-down asymmetry. At $R=20\,000$, the boundaries of the resulting 1-cells vibrate.

For $P=7$ and $R=12\,000$, we observed transformations that either ended in state (d) ($k_0=1.2$ or 1.35) or demonstrated a final transition (d)→(l) ($k_0=1.5$). At $k\gtrsim 2$, stable stellate 1-cells (b) were formed.

Four scenarios were run at $P=1$, $R=18\,000$. In three of them, the final state was time dependent, represented by unsteady rolls. They were either slightly turbulent ($k_0=0.8$) or superposed with asymmetric running waves ($k_0=1$ and 1.2). At $k_0=1$, a kaleidoscopic stage (b′) preceded the formation of two-vortex cells, which then transformed into 2-cells and ultimately led to state (c′). State (k) was found to be final in the run for $k_0=1.4$. At $P=1$, all the *d* runs yielded scenarios very similar to those observed in the corresponding runs of the basic series.

To summarize, we note that the features of the observed scenarios agree with the idea of the general tendency of the flow seeking its optimum scale. Of particular interest are two-vortex hexagons with a reduced characteristic flow scale. If short-wave hexagons are stable, they exhibit a specific, stellate fine structure. Conditions for the realizability of the revealed patterns or some of their features under natural conditions still remain, however, to be explored.

We are grateful to W. Pesch for the availability of the numerical code and to F. H. Busse for valuable discussions. The work of A.V.G. was supported by the German Academic Exchange Service and by the Russian Foundation for Basic Research (Project No. 00-02-16313).

[1] M. Assenheimer and V. Steinberg, Phys. Rev. Lett. **76**, 756 (1996).
[2] R.M. Clever and F.H. Busse, Phys. Rev. E **53**, R2037 (1996).
[3] F.H. Busse and R.M. Clever, Phys. Rev. Lett. **81**, 341 (1998).
[4] F. H. Busse and R. M. Clever, in *Les Phenomenes Critiques au Chaos*, edited by P. Manneville (DRECAM/SPEC, CEA, Saclay, 1999), pp. 79–92.
[5] A. V. Getling, *Rayleigh-Bénard Convection: Structures and Dynamics* (World Scientific, Singapore, 1998).
[6] W. Pesch, Chaos **6**, 348 (1996).